Performance of terrestrial laser scanning to characterize managed Scots pine (*Pinus sylvestris* L.) stands is dependent on forest structural variation

Tuomas Yrttimaa [a,b], Ninni Saarinen [b,a], Ville Kankare [a,b], Jari Hynynen [c], Saija Huuskonen [c], Markus Holopainen [b,d], Juha Hyyppä [d], Mikko Vastaranta [a]

[a] School of Forest Sciences, University of Eastern Finland, Joensuu, 80101, Finland

[b] Department of Forest Sciences, University of Helsinki, Helsinki, 00014, Finland

[c] Natural Resources Institute Finland (Luke), Helsinki, 00790, Finland

[d] Department of Remote Sensing and Photogrammetry, Finnish Geospatial Research Institute, National Land Survey of Finland (NLS), Masala, 02431, Finland

Correspondence to: Tuomas Yrttimaa [a,b] (tuomas.yrttimaa@uef.fi)

Abstract

There is a limited understanding of how forest structure affects the performance of methods based on terrestrial laser scanning (TLS) to derive tree and forest structural attributes. We aim to improve the understanding of how different forest management activities that shape tree size distributions affect the TLS-based forest characterization accuracy in managed Scots pine (*Pinus sylvestris* L.) stands. For that purpose, we investigated 27 sample plots consisting of three different thinning types, two thinning intensities as well as control plots without any treatments. Multi-scan TLS point clouds were collected from the sample plots, and a point cloud processing algorithms were used to segment individual trees and classify the segmented point clouds into stem and crown points that were further used to measure tree attributes. Finally, the forest structural attributes were aggregated from the derived tree attributes. With the TLS-based forest characterization, almost 100% completeness in tree detection, 0.7 cm (3.4%) root-mean-square-error (RMSE) in diameter-at-breast-height measurements, 0.9-1.4 m (4.5-7.3%) RMSE in tree height measurements, and less than 6% relative RMSE in estimates of forest structural attributes (i.e. mean basal area, number of trees per hectare, mean volume, basal-area weighted mean diameter and - height) were obtained depending on the applied thinning type. Thinnings decrease variation in horizontal and vertical forest structure which favoured TLS-based tree detection and tree height measurement, enabling reliable estimates for forest structural attributes. Considerably lower performance was recorded for control plots without any treatments. Thinning intensity was noticed to affect more on the accuracy of TLS-based forest characterization than thinning type. Number of trees per hectare and the proportion of suppressed trees were recognized as the main factors affecting the accuracy of TLS-based forest characterization. The more variation there was in the tree size distribution, the more challenging it was for the TLS-based method to capture all the trees and measure the tree and forest structural attributes. In general, consistent and reliable tree and forest attributes can be expected when using TLS for characterizing managed boreal forests.

Keywords: LiDAR, remote sensing, forest inventory, point cloud, close-range, forest management

INTRODUCTION

Terrestrial laser scanning (TLS) is a powerful close-range sensing method for characterizing forests in three dimensions (3D; Dassot et al., 2011; Liang et al., 2016; Newnham et al., 2015; Yrttimaa, Saarinen, Kankare, et al., 2019; Yrttimaa, Saarinen, Luoma, et al., 2019). Individual trees can be detected from a TLS point cloud by detecting circular shapes (e.g. (Aschoff et al., 2004; Maas et al., 2008) or clusters of points (e.g. Cabo et al., 2018; Zhang et al., 2019), these two represent the most common tree detection methods implemented in forest applications (Liang et al., 2016). Then, depending on the algorithm used and the purpose of the processing, architectural structure of a stem (Heinzel & Huber, 2016; Liang et al., 2012) or a whole tree (Hackenberg et al., 2014; Raumonen et al., 2013) can be reconstructed by using a series of geometrical primitives, preferably circular cylinders (Åkerblom et al., 2015). Tree reconstruction requires that

points representing a tree are classified based on their origin, in other words from stem, branches, and foliage. Point cloud classification algorithms are most often based on an assumption that stem points have more planar, vertical and cylindrical characteristics than points originating from branches and foliage (Liang et al., 2012; Olofsson & Holmgren, 2016; Raumonen et al., 2013; Yrttimaa, Saarinen, Kankare, et al., 2019). With careful TLS data collection and preprocessing, single point in TLS data can reach a millimeter-level accuracy within the data set (Liang et al., 2018; Wilkes et al., 2017) meaning that reconstructed tree models are geometrically highly accurate (Hackenberg et al., 2014). So far, there exists a limited number of approaches for classifying points originating from foliage, but laser return intensity, for example, could presumably be used for separating foliage and wooden parts (Junttila et al., 2019). After tree architecture is reconstructed for every tree in an area of interest, theoretically all external tree dimensions can be derived from geometrically accurate 3D models for all the trees and used further in deriving attributes of interest.

It is known that the accuracy of forest characterization with TLS depends on the scanning setup, tree detection algorithm, algorithm for reconstructing tree structure, and completeness of a point cloud (i.e. visibility of trees in a point cloud; (Liang et al., 2018)). Occlusion, causing incompleteness of a point cloud, is seen as the main source of error (Abegg et al., 2017; Yrttimaa, Saarinen, Kankare, et al., 2019) limiting the feasibility of TLS in forest characterization. Occlusion effects are twofold. First, some of the trees remain undetected which causes bias to the derived forest structural attributes, such as basal area and growing stock volume. Second, tree architectural structure cannot be fully reconstructed due to limited number of points characterizing a tree and this is causing errors to the derived tree attributes, such as stem form and height. Currently, there is a limited understanding of how forest structure affects the occlusion and further on the derived tree and forest structural attributes. At the general level, it is known that the amount of undergrowth vegetation, tree density, basal area, tree species, tree size distribution, and the amount of branches all affect how well TLS is capable of characterizing a forest, but controlled experiments are lacking. Furthermore, it is not known how much there is variation in accuracy of TLS-based forest characterization within similar kind of forest conditions (i.e. density, basal-area, the amount of undergrowth vegetation) or how different forest management activities (i.e. different thinning types and intensities vs no management) that shape tree size distribution affect the TLS-based forest characterization accuracy. When TLS is increasingly used in investigating, mapping and monitoring managed forests its expected accuracy is imperative to be known.

The objective of this study is to examine how forest structure and especially different thinning treatments affect TLS-based forest characterization. We investigated the accuracy of TLS-derived tree and forest structural attributes using sample plots with controlled variation in forest structure. In our study design, we standardized the effect of 1) forest structure by placing sample plots into stands that were harvested for research purposes with varying thinning type and intensity, 2) tree species by investigating pure Scots pine (*Pinus sylvestris* L.) stands, 3) scanning setup by using similar multi-scan approach for all of the sample plots, 4) amount of undergrowth vegetation as it was removed from all the sample plots, and 5) algorithm by using state-of-the-art techniques (Yrttimaa, Saarinen, Kankare, et al., 2019). We aim to improve understanding of how different thinning treatments that are aimed at shaping tree size distribution affect the TLS-based forest characterization accuracy in Scots pine stands. For that purpose, we studied three thinning types along with two thinning intensities as well as control plots without any treatments. In addition, we investigated how consistent results can be obtained for tree and forest structural attributes in similar forest conditions (i.e. by analysing the accuracy among sample plots with the same thinning type and intensity) with TLS-based point clouds.

MATERIALS AND METHODS

Study materials

Study site and experimental design

The study materials consist of field-measured tree inventory data and multi-scan TLS point cloud data collected from three study sites located in southern Finland (62°4.4'N 24°30.1'E, 62°3.6'N 24°19.9'E, and

61°21.8'N 25°6.3'E) representing managed, even-aged Scots Pine dominated forest stands at the age of around 50 years. Nine rectangular sample plots (1000-1200m^2) were established for each study site in 2005 or 2006 by Natural Resources Institute Finland (Luke) making 27 sample plots in total. The experimental design of the sample plots includes three thinning types (i.e. thinning from below, thinning from above, systematic thinning from above) with two levels of thinning intensity (i.e. moderate, intensive) resulting in six different thinning treatments (Saarinen et al., 2020).

Thinning types represent different approaches to determine the trees to be removed. In thinning from below suppressed and co-dominant trees were removed whereas in thinning from above mostly dominant trees were removed. In both thinning types, small and damaged trees were also removed and the regular spatial distribution of the trees were maintained. In systematic thinning from above, only dominant trees were removed without considering the regularity of spatial distribution of remaining trees. Thinning intensity refers to the proportion of basal area (m^2/ha) removed in thinning. Moderate thinning refers to prevailing thinning guidelines applied in Finland (Rantala, 2011) whereas intensive thinning corresponds 50% lower remaining basal area than in the plots with moderate thinning intensity.

At the time of establishment, the thinning treatments were applied for 24 sample plots to make three to five repetitions of each treatment in total. One sample plot from each study site was chosen as a control plot with no treatments carried out since the establishment. Due to different treatments and the trees' ability to adapt to changes in growth resources, the forest structure of the sample plots have developed differently from similar starting conditions since the time of establishment (Table 1).

Field inventory

Tree-wise field inventory was carried out in October 2018 and April 2019 to obtain reference measurements for all the 2204 trees within the sample plots. Tree species, diameter at breast height (dbh) from two perpendicular directions, crown layer, and health status were recorded from each tree within a plot (tally trees). About half of the trees (928) were selected as sample trees from which tree height, crown base, and height of the lowest dead branch were also measured using electronic clinometer. Heights of the tally trees were estimated using allometric models that were calibrated for each sample plot using the sample trees. Stem volume was estimated for all the trees from dbh and tree height using nationwide, species-specific volume equations (Laasasenaho, 1982). The plot-level forest structural attributes were then aggregated based on the tree attributes.

Table 1. Variation in forest structural attributes on the sample plots by thinning types and intensities based on field inventory data acquired in October 2018 and April 2019. D_g = basal area-weighted mean diameter (cm), H_g = basal area-weighted mean height (m), G = mean basal area (m^2/ha), TPH = trees per hectare (n/ha), V_{mean} = mean volume (m^3/ha), mod. = moderate thinning intensity, and int. = intensive thinning intensity.

Forest structural attribute	Thinning type	Minimum (mod. / int.)	Mean (mod. / int.)	Maximum (mod. / int.)	Standard Deviation (mod. / int.)
D_g (cm)	Thinning from below	21.0 / 25.5	23.5 / 27.5	25.3 / 31.1	2.2 / 3.1
	Thinning from above	18.4 / 19.7	21.2 / 22.3	22.8 / 24.9	1.9 / 2.1
	Systematic thinning	19.0 / 17.7	20.6 / 22.2	21.6 / 25.1	1.2 / 3.0
	Control	18.1	21.0	23.8	2.9
H_g (m)	Thinning from below	19.4 / 20.5	21.7 / 21.6	23.2 / 23.5	2.0 / 1.6
	Thinning from above	19.8 / 18.1	21.0 / 19.5	22.2 / 20.7	1.1 / 1.2
	Systematic thinning	18.5 / 16.9	20.3 / 20.0	22.2 / 21.9	1.4 / 2.2
	Control	18.2	21.4	24.6	3.2

G (m^2/ha)	Thinning from below	26.9 / 15.4	28.4 / 15.9	31.3 / 16.7	2.5 / 0.7
	Thinning from above	27.0 / 15.2	28.3 / 16.1	29.2 / 17.8	0.9 / 1.2
	Systematic thinning	25.0 / 13.3	27.5 / 15.8	29.3 / 17.7	1.6 / 1.8
	Control	33.6	37.7	43.3	5.1
TPH (n/ha)	Thinning from below	625 / 215	705 / 287	835 / 340	113 / 65
	Thinning from above	747 / 336	917 / 446	1229 / 528	213 / 82
	Systematic thinning	804 / 320	945 / 462	1083 / 742	111 / 174
	Control	1240	1312	1448	118
V_{mean} (m^3/ha)	Thinning from below	251.0 / 151.5	291.8 / 160.8	339.7 / 169.6	44.8 / 9.1
	Thinning from above	273.8 / 133.1	282.5 / 150.5	289.0 / 160.8	6.4 / 12.6
	Systematic thinning	245.9 / 133.8	267.0 / 149.3	283.0 / 162.4	14.4 / 11.6
	Control	297.7	388.9	501.2	103.4

Terrestrial laser scanning data acquisition

The TLS data were collected using Trimble TX5 (Trimble Inc., Sunnyvale, California, United States) phase-shift scanner that operates at a 1550 nm wavelength and measures 976,000 points per second, delivering a hemispherical (300° vertical x 360° horizontal) point cloud with an angular resolution of 0.009° in both vertical and horizontal direction. Multi-scan approach was used in the TLS campaign to ensure point cloud quality. The scanning setup consisted of two center scans placed a few meters apart from each other near the plot center, and six auxiliary scans placed closer to the plot borders making eight scanning locations in total (Saarinen et al., 2020) (see Fig. 1). Artificial reference targets were used to register and merge the point clouds from each scanning location together following similar procedure used in e.g. (Yrttimaa, Saarinen, Luoma, et al., 2019).

Deriving tree and forest structural attributes from point clouds

General description

A modified version of the point cloud processing method presented in (Yrttimaa, Saarinen, Kankare, et al., 2019) was used in this study to segment trees, classify the point cloud into stem and crown points, and to measure tree attributes from the multi-scan TLS point clouds. Finally, the forest structural attributes were aggregated from the derived tree attributes. The outline of the method is presented in Fig. 1 and explained in detail in the following sections.

Canopy segmentation

First raster-based canopy segmentation was carried out to partition the point clouds into smaller areas to speed up the computations in further stages of the processing workflow (Fig. 1 a). Canopy height models (CHMs) at a 20 cm resolution were generated from the normalized point clouds using the LAStools software (Isenburg, 2019). Variable Window Filter approach (Popescu & Wynne, 2004) was used to identify the local maximas in CHMs, and Marker-Controlled Watershed Segmentation (Meyer & Beucher, 1990) was applied to delineate the canopy segments. The point clouds were then split according to the extracted crown segments using point-in-polygon approach.

Point cloud classification

At this point it is assumed that each crown segment may contain multiple trees if the crowns of adjacent trees are overlapping. These trees were separated from each other and the segmented point clouds were further classified into stem points and non-stem points using the point cloud classification approach developed in this study (Fig. 1 b). The classification was based on a general assumption that stem points have more planar, vertical and cylindrical characteristics than points representing branches and foliage (Liang et al., 2012; Yrttimaa, Saarinen, Kankare, et al., 2019). The proposed method is an iterative procedure that begins from the base of a tree stem and proceeds towards the tree top. Thus, the tree segment is first partitioned into n number of horizontal point cloud slices $P_1 \dots P_n$. The first slice, P_1 is delineated between the heights of 0 m and 4 m to access the stem origin. From P_2 upwards the point cloud is binned at 50 cm vertical intervals until the tree top is reached. For each point cloud bin the following procedure is repeated to identify stem points and non-stem points: 1) Grid average downsampling, 2) Surface normal filtering, 3) Point clustering, 4) Random sample consensus (RANSAC)-cylinder filtering, and 5) Stem points and non-stem points extraction.

The binned point cloud is first sampled to uniform the point spacing using grid-average-downsampling method with a grid size of 5 mm. Surface normal vectors were computed for the downsampled points according to their 40 neighbour points to extract points on vertical surfaces (i.e. horizontal normal vector orientation). Vertical surface points were then segmented into clusters with a minimum of 30 cm Euclidean distance between points from different clusters. It is assumed that stem points compose of larger vertical clusters compared to non-stem points. Thus, clusters that contain the minimum acceptable number of points m and have a vertical dimension exceeding the set minimum value k are classified as candidate stem points. The values for m and k were 100 points and 1 m for P_1 and 40 points and 30 cm for $P_2 \dots P_n$. Values for these parameters should be set based on the realized point cloud density and *a prior* knowledge on tree height range. However, it should be noted that in our preliminary investigations, the method was not sensitive to the used parameter values. Due to overlapping canopies there might be multiple trees inside a tree segment. Therefore in case of P_1 the point cloud clustering procedure is repeated using a 50 cm Euclidean distance threshold to separate those trees from each other.

RANSAC-cylinder filtering procedure (Yrttimaa, Saarinen, Kankare, et al., 2019) was then applied for the candidate stem points to ensure that the identified stem point clusters represent the cylindrical form of a tree stem. An alpha shape was created to envelope the identified stem points. Points of the original, non-sampled point cloud bin that fell inside the alpha shape were classified as stem points while points that fell outside the alpha shape were classified as non-stem points. After completing the classification in bin P_i, the procedure proceeded to bin P_{i+1} where the parameters of the fitted RANSAC-cylinder in P_i were used to guide the point classification.

Tree attribute extraction and aggregation of plot-level forest structural attributes

Tree attributes, namely dbh, tree height, and stem volume, were extracted from the classified point clouds following the procedure originally presented in (Yrttimaa, Saarinen, Kankare, et al., 2019) (Fig. 1 c). Tree height was determined as the vertical distance between the highest and lowest points for each tree. Stem taper curve was estimated by measuring diameters through circle fitting at 20 cm vertical intervals to the stem points. The outliers in diameter-height -observations were filtered out by comparing the measured diameters to the mean of three previous (or three closest at the bottom of the stem) diameters. Then a cubic spline curve was fitted to the diameter-height -observations to level unevenness in diameter measurements and to interpolate the missing diameters as in (Saarinen et al., 2017). Dbh was then obtained as the diameter at 1.3 m height from the taper curve. Stem volume was estimated using Huber formula by considering the stem as a sequence of vertical cylinders (Fig. 1 c).

Finally, the plot-level forest structural attributes, mean basal area (G, m^2/ha), number of trees per hectare (TPH, n/ha), mean volume (V_{mean}, m^3/ha), basal-area weighted mean diameter (D_g, cm) and - height (H_g, m) were computed from tree attributes.

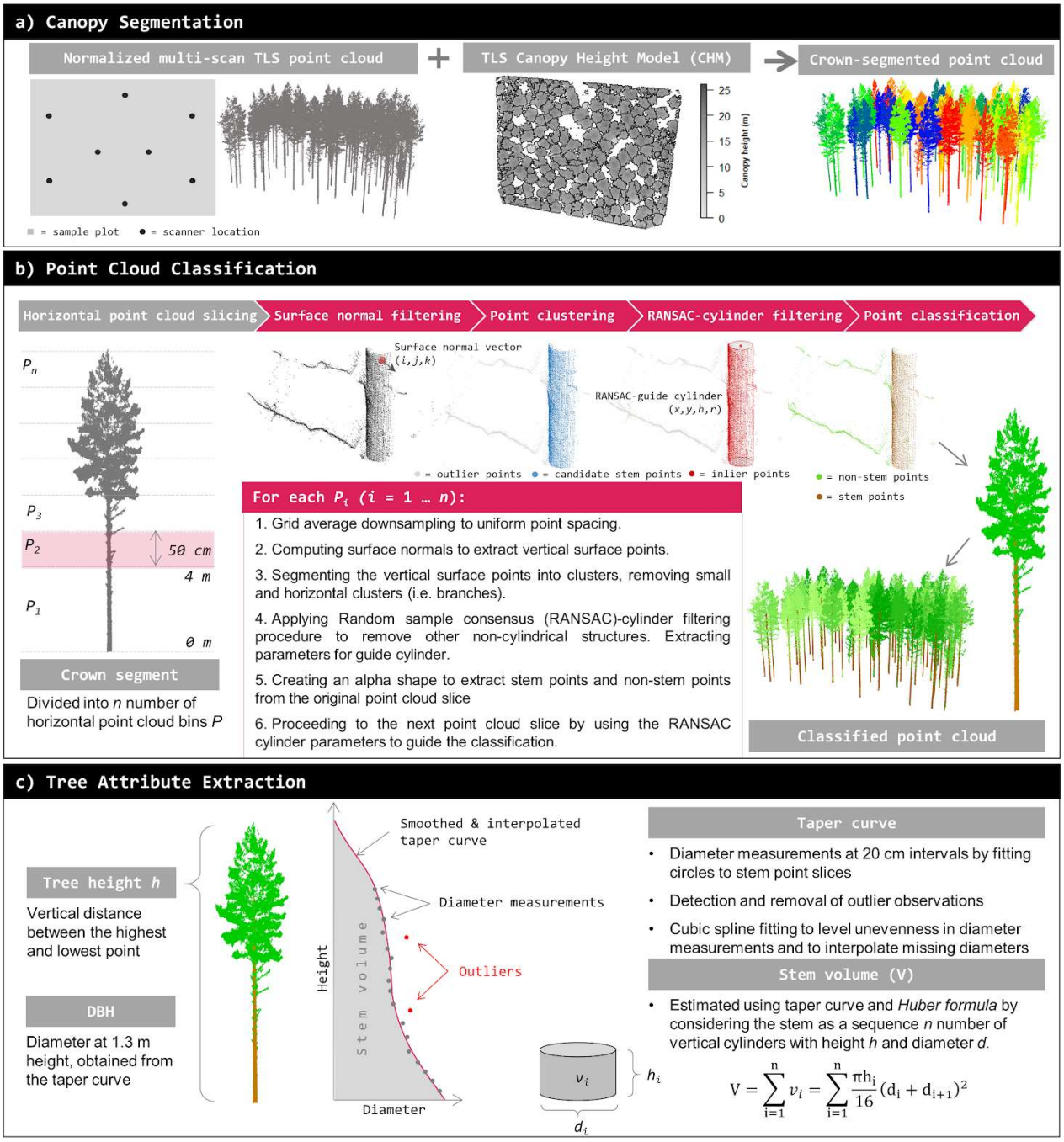

Fig. 1. Outline how tree and forest structural attributes were derived from the terrestrial laser scanning (TLS) point clouds.

Assessing the performance of the TLS-based forest characterization

Performance of the TLS-based method to characterize forest structure was assessed by comparing the TLS point cloud-derived tree attributes (dbh and tree height) and plot-level forest structural attributes (D_g, H_g, G, TPH, V_{mean}) with the field-measured ones by using bias (mean error) and root-mean-square-error (RMSE) as accuracy measures:

$$bias = \frac{\sum_{i=1}^{n}(\hat{X}_i - X_i)}{n} \quad (1)$$

$$RMSE = \sqrt{\frac{\sum_{i=1}^{n}(\hat{X}_i - X_i)^2}{n}} \quad (2)$$

where n is the number of sample plots, $\widehat{X}_i$ is the TLS point cloud-derived tree attribute or forest structural attribute for plot i, and X_i is the corresponding attribute based on validation measurements.

Accuracy of the TLS-based forest characterization is affected by the capability of the method to detect trees from the point clouds (Liang et al., 2018; Yrttimaa, Saarinen, Kankare, et al., 2019). Therefore, we also analysed the tree detection accuracy at plot level using completeness and correctness as accuracy measures. Completeness indicates the percentage of trees detected from the point clouds, whereas correctness measures the percentage of TLS-derived trees that were correctly matched with the reference. At plot level, completeness indicates the tree detection rate, or how large a part of the field-measured TPH is detected from the point clouds.

To reveal the effects of thinning treatments on the performance of the TLS-based forest characterization, the accuracy was assessed by thinning type and intensity. One-sample *t*-test was used in pairwise investigations to examine whether the estimation error of tree and forest structural attributes in one treatment type significantly differed from the errors of the respective estimates of another treatment types.

In addition, we investigated how consistent results can be obtained with TLS for tree and forest structural attributes in similar forest conditions by analysing the variation in accuracy measures among sample plots with the same thinning type and intensity and comparing the range of variation in accuracy measures between different treatment types.

RESULTS

Overall performance

Out of the total number of 2102 Scots pine trees, 2076 (98.8%) were automatically detected from the TLS point clouds. The stem volume of the detected trees accounted for 99.5% of the total stem volume of the trees. Suppressed trees accounted for 48.2% of the trees that remained undetected from the points clouds, while the respective proportion in the whole tree population was only 4.5%. Correctness of tree detection was 100% indicating robust performance of the TLS-based method in managed Scots pine forests.

On average, dbh and tree height of all the trees were underestimated by 0.1 cm and 0.3 m, respectively. RMSE in dbh measurements was 0.7 cm (3.4%) while in tree height measurements the RMSE was 1.6 m (8.4%). Accuracy in tree attribute extraction was similar for dominant and co-dominant trees while for suppressed trees the dbh (RMSE 9.3%) and tree height (RMSE 18.5%) were measured less accurately.

Relative RMSEs of < 5.5% were recorded for all the forest structural attributes considering all the sample plots (Table 1). On average, V_{mean} was overestimated while the other attributes were underestimated. Erroneous tree height measurements seemed to compensate at the plot level as the H_g was estimated more accurately than the individual tree heights.

The effects of thinning treatment on the performance of TLS-based approach

Overall completeness in tree detection was at the same level for all the thinning types: 100% for thinning from below, 99.7% for thinning from above, and 99.4% for systematic thinning. Tree detection accuracy slightly decreased when no treatments were applied on the sample plots being 95.6% for the control plots. No significant differences ($p > 0.05$) in tree detection accuracy was noticed between different thinning types, including control plots (Figs. 2-3). Field-measured and TLS-estimated dbh distributions (Fig. 2a-g) and tree height distributions (Fig. 3a-g) were similar regardless of different thinning treatments. The few trees that remained undetected from the control plots mainly represented the small dbh and height classes (Figs. 2g, 3g).

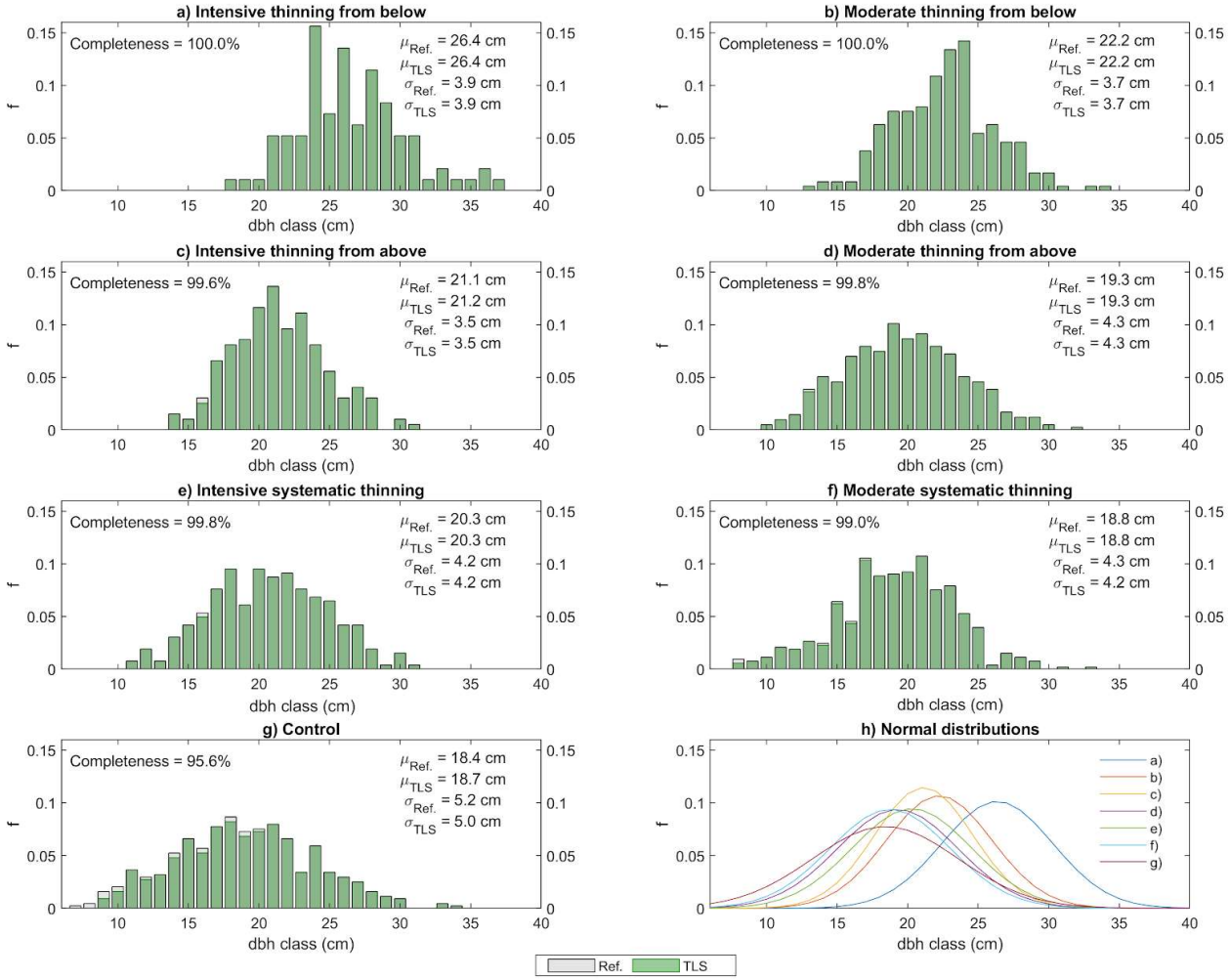

Fig. 2. Diameter-at-breast-height (dbh) distributions for each thinning treatment (a-g). Coloured bars represent the proportion of trees that were detected from the terrestrial laser scanning point clouds. For comparison, the dbh distributions are described as normal distributions with parameters (μ = mean value, σ = standard deviation) extracted from the field-measured dbh distributions.

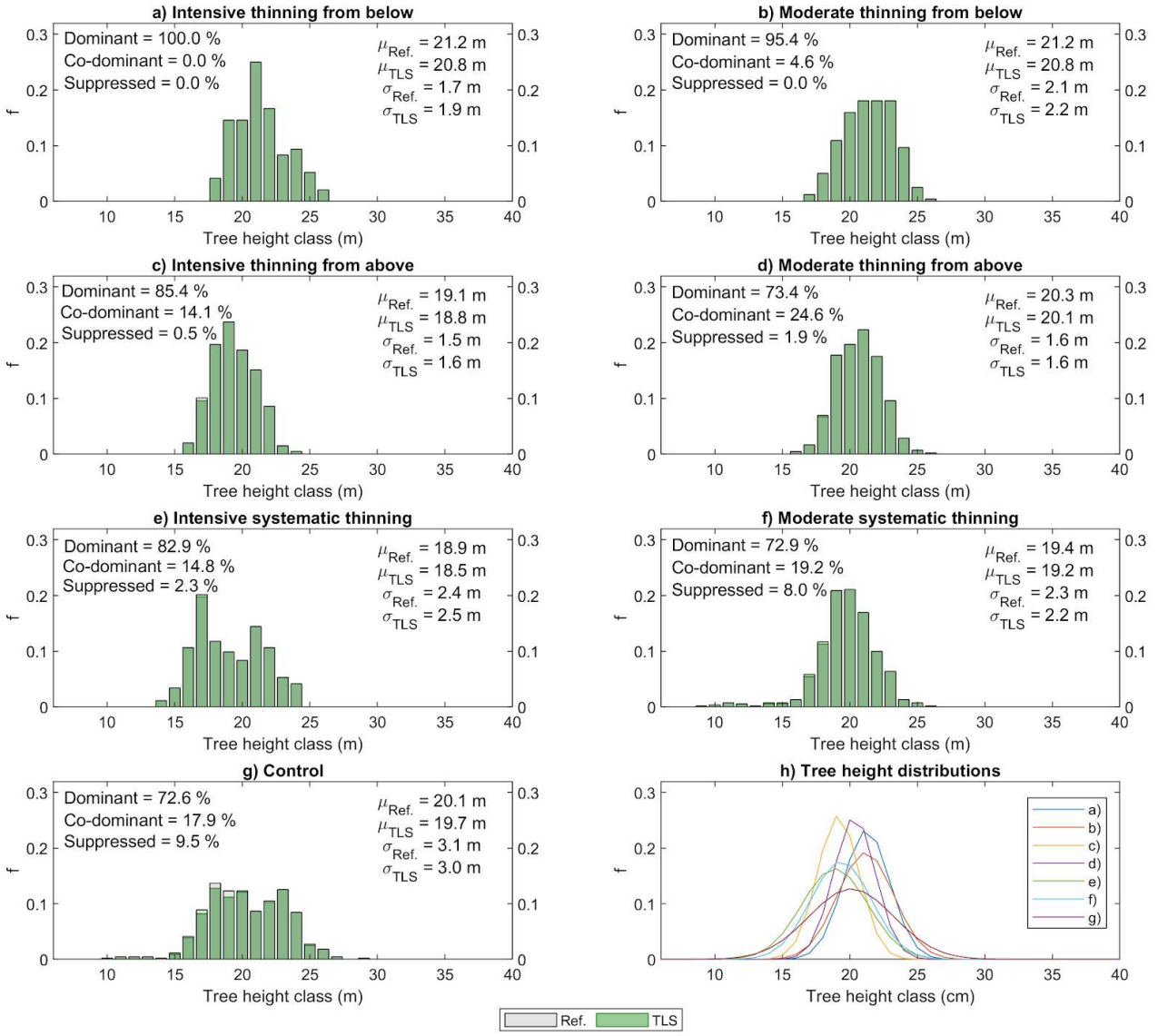

Fig. 3. Tree height distributions and proportions of trees on different canopy layers for each thinning treatment (a-g). Coloured bars represent the proportion of trees that were detected from the terrestrial laser scanning point clouds. For comparison, the tree height distributions are described as normal distributions with parameters (μ = mean value, σ = standard deviation) extracted from the field-measured height distributions.

Accuracy in dbh measurements remained consistent throughout the sample plots from different treatments (Table 2). Instead, accuracy in tree height measurements slightly varied by the treatment. Bias in tree height measurements was at the same level for thinning from below and control plots, and for thinning from above and systematic thinning. RMSE in tree height measurements varied between 0.89 m to 2.22 m being lowest for thinning from above and highest for control plots, while reaching the same level for thinning from below and systematic thinning.

D_g was estimated with similar accuracy throughout the different thinning treatments (inc. control plots), while the accuracy of estimates for other forest structural attributes varied more between different thinning treatments (Table 2). Accuracy of the estimates for H_g, G, TPH and V_{mean} differed when comparing the accuracy measures from control plots with the other plots. No significant differences ($p > 0.05$) in accuracy for H_g, G and V_{mean} estimates were recorded between thinning from above, thinning from below and systematic thinning (Table 2). In the case of TPH, the highest accuracy was recorded for thinning from below whereas the accuracy was similar for both thinning from above and systematic thinning.

Table 2. Bias and root-mean-square-error (RMSE) of estimates of tree and forest structural attributes on sample plots from different thinning types. Negative bias denotes underestimation. The highlighted *p*-values < 0.05 indicate significant differences in the mean errors of the tree/forest attribute estimates between sample plots from different thinning types. dbh = diameter-at-breast-height, D_g = basal area-weighted mean diameter (cm), H_g = basal area-weighted mean height (m), G = mean basal area (m^2/ha), TPH = trees per hectare, (n/ha) and V_{mean} = mean volume (m^3/ha).

Tree / Forest Attribute		Accuracy measures		Significance of error differences between thinning types (*p*-values)			
	Thinning type	**Bias**	**RMSE**	*Below*	*Above*	*Syst.*	*Control*
dbh (cm)	Thinning from below	-0.20 (-0.8%)	0.70 (3.0%)	1	0.056	**0.009**	**0.000**
	Thinning from above	-0.13 (-0.6%)	0.63 (3.2%)	-	1	0.285	**0.004**
	Systematic thinning	-0.10 (-0.5%)	0.65 (3.4%)	-	-	1	**0.044**
	Control	-0.06 (-0.3%)	0.76 (4.1%)	-	-	-	1
Tree height (m)	Thinning from below	-0.42 (-2.0%)	1.28 (6.1%)	1	**0.045**	**0.014**	0.362
	Thinning from above	-0.28 (-1.4%)	0.89 (4.5%)	-	1	0.359	**0.000**
	Systematic thinning	-0.25 (-1.3%)	1.41 (7.3%)	-	-	1	**0.000**
	Control	-0.48 (-2.4%)	2.22 (11.0%)	-	-	-	1
D_g (cm)	Thinning from below	-0.34 (-1.3%)	0.43 (1.7%)	1	0.460	0.251	0.092
	Thinning from above	-0.24 (-1.1%)	0.30 (1.4%)	-	1	0.399	0.053
	Systematic thinning	-0.18 (-0.9%)	0.31 (1.4%)	-	-	1	0.269
	Control	0.09 (0.4%)	0.23 (1.1%)	-	-	-	1
H_g (m)	Thinning from below	-0.46 (-2.1%)	0.55 (2.6%)	1	0.480	0.856	**0.049**
	Thinning from above	-0.35 (-1.7%)	0.45 (2.2%)	-	1	0.486	**0.004**
	Systematic thinning	-0.43 (-2.1%)	0.46 (2.3%)	-	-	1	**0.000**
	Control	-0.82 (-3.8%)	1.07 (5.0%)	-	-	-	1
G (m^2/ha)	Thinning from below	-0.50 (-2.3%)	0.64 (2.9%)	1	0.982	0.603	**0.002**
	Thinning from above	-0.51 (-2.3%)	0.57 (2.5%)	-	1	0.322	**0.000**
	Systematic thinning	-0.41 (-1.9%)	0.51 (2.4%)	-	-	1	**0.000**
	Control	-1.58 (-4.2%)	1.70 (4.5%)	-	-	-	1
TPH (n/ha)	Thinning from below	-1.35 (-0.3%)	3.31 (0.7%)	1	**0.029**	**0.003**	**0.000**
	Thinning from above	-5.44 (-0.8%)	8.25 (1.2%)	-	1	0.246	**0.000**
	Systematic thinning	-8.41 (-1.2%)	13.40 (1.9%)	-	-	1	**0.000**
	Control	-82.32 (-6.3%)	98.67 (7.5%)	-	-	-	1
V_{mean} (m^3/ha)	Thinning from below	6.24 (2.8%)	13.36 (5.9%)	1	0.804	0.907	**0.022**
	Thinning from above	7.62 (3.5%)	10.37 (4.8%)	-	1	0.789	**0.000**
	Systematic thinning	6.88 (3.3%)	11.21 (5.4%)	-	-	1	**0.000**
	Control	-11.04 (-2.8%)	20.36 (5.2%)	-	-	-	1

Consistency of TLS-based measurements in similar forest conditions

Variation in tree detection accuracy on sample plots within the same thinning treatment remained consistent (Fig. 4h). Range of variation in tree detection rate (i.e. completeness) within similar forest conditions (i.e. same thinning type and intensity) varied from 0.0% to 2.3% on treated sample plots. When no thinning treatments were carried out the range of variation in tree detection rate was considerably larger being 8.2% for the control plots.

Variation in dbh measurement error was similar regardless of the applied thinning type or intensity (Fig. 4a). For tree height measurements, smaller variation in measurement error was recorded in intensively thinned sample plots (Fig. 4b). Range of variation in tree height measurement error was the largest on sample plots with most variation in tree size distribution (i.e., control plots and sample plots with moderate systematic thinning, see Figs. 2f-g, 3f-g).

Variation in errors in D_g estimates on sample plots within the same treatment remained consistent (Fig. 4c). When estimating H_g, G, TPH, and V_{mean}, the variation in estimation errors between sample plots from the same treatment was significantly ($p < 0.05$) smaller on thinned plots than on control plots (Fig. 4d-g). The error in G and V_{mean} estimates varied less within the sample plots with intensive thinning. The same applies with H_g except for sample plots with thinning from above where moderate thinning intensity resulted in smaller variation in the estimation errors (Fig. 4d).

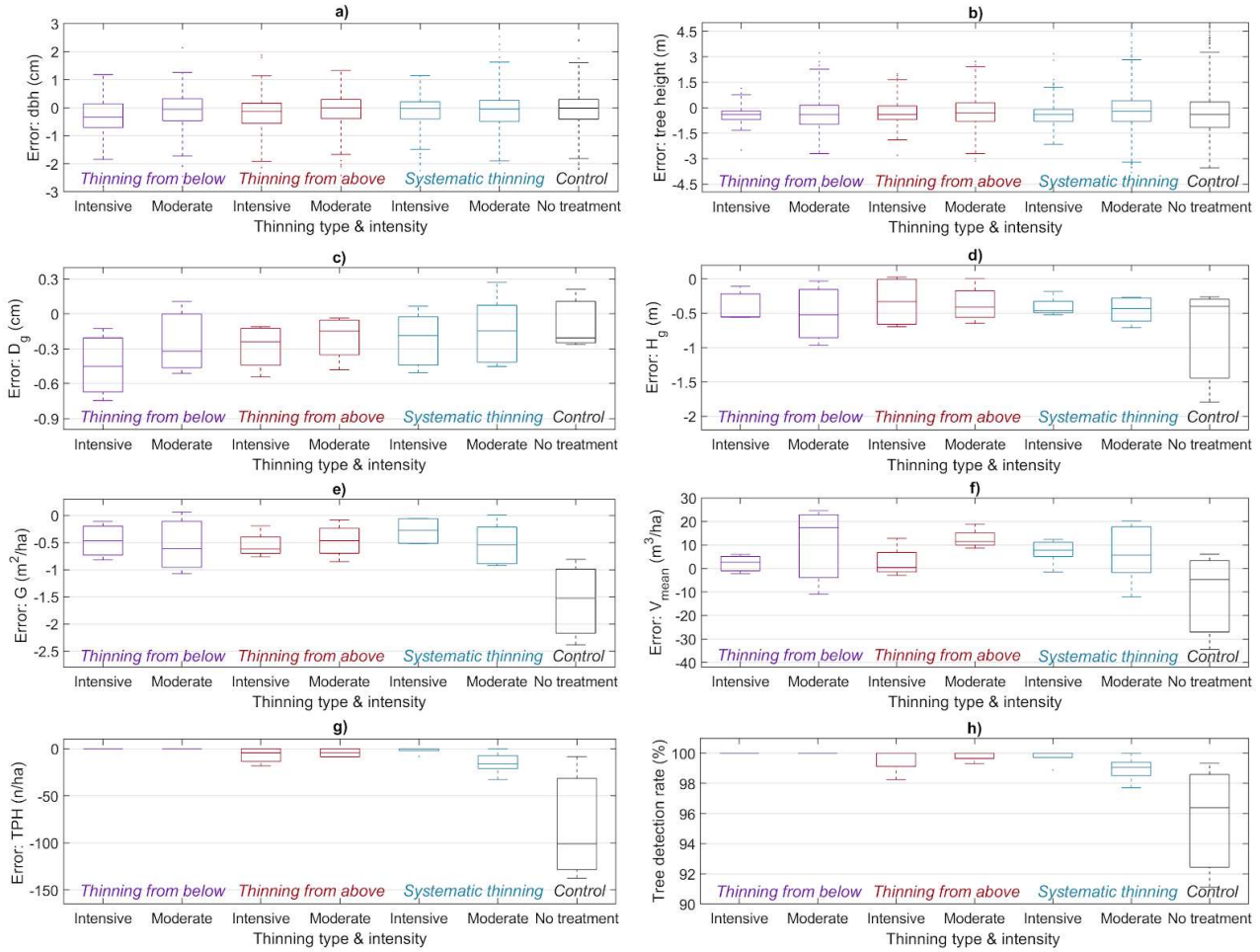

Fig. 4. Variation in estimation errors in tree attributes (a-b), estimation errors of plot-level forest structural attributes (c-g) and tree detection rate (h) within and between thinning treatments.

DISCUSSION

The objective of this study was to examine the effects of different thinning treatments on the performance of multi-scan TLS-based forest characterization in managed Scots pine forest stands. Different thinning treatments implemented to similar forest stands (2005 and 2006) resulted in different forest structures 13 growing seasons later (Figs. 2-3). According to the results of this study, accuracy of using the TLS-based approach for detecting trees, measuring tree heights and estimating forest structural attributes (i.e. H_g, TPH, G, and V_{mean}) varied between the treatments due to differences in tree size distributions (Table 2). Thinning treatments in general explained most of the variation in the accuracy measures between all the sample plots. For control plots where no thinnings were carried out the accuracy was at a lower level and varied more among the sample plots than it did for sample plots with thinning treatments (Fig. 4). The TLS-based approach provided the most consistent estimates for H_g, G, and V_{mean} for intensively thinned sample plots.

Forests were characterized accurately when the TLS-based method was applied for managed Scots pine stands where forest management activities had been carried out. Almost 100% completeness in tree detection, 0.7 cm RMSE in dbh measurements, and 0.9-1.4 m RMSE in tree height measurements were obtained depending on the applied thinning type (Table 2). These results are in line with the previous findings on the performance of TLS-based methods in characterizing trees on stands with relatively simple forest structure. Based on the existing knowledge, almost all the trees can be detected and dbh measured with an accuracy of a few centimeters when the TLS-based method is applied to single-layered temperate (Bauwens et al., 2016; Koreň et al., 2017; Ritter et al., 2017) or boreal forests (Liang et al., 2018; Olofsson & Holmgren, 2016; Saarinen et al., 2017). However, measuring tree height correctly with multi-scan TLS has been recognized as the major challenge due to the hemispherical scanning geometry and thus, several meters of error in tree height measurements of conifers in boreal forests can be expected (Liang et al., 2018, 2016; Wang et al., 2019). Nevertheless, the results of this study demonstrate that also tree height can be measured reliably when there is adequate visibility from the scanner to the treetops. Considering the accuracy of tree attribute measurements, it should be noted that the accuracy obtained here with the TLS-based approach was close to the realized precision of the reference measurements as precision of 0.3 cm for dbh and 0.5 m for tree height are expected in similar boreal forest conditions when calipers and clinometers were used (Luoma et al., 2017).

Tree detection rate and tree height measurement accuracy varied between the sample plots due to variation in horizontal and vertical forest structure. Tree detection accuracy was noticed to decrease especially when no thinnings were carried out. It is known that tree detection accuracy is mostly affected by occlusion which is caused by vegetation (Abegg et al., 2017; Yrttimaa, Saarinen, Kankare, et al., 2019), since trees behind other trees and bushes cannot be recorded. The use of multi-scan setup decreases the number of occluded trees (Bauwens et al., 2016; Liang et al., 2016), but with fixed scanning setup and the lack of undergrowth vegetation in the study sites, variation in tree detection accuracy between the sample plots is explained mainly by variations in tree size distributions. According to the results of this study, most of the trees that were not detected were small (in terms of dbh and height) and suppressed, meaning that they were located next to a larger dominant tree. The smaller the tree is, the less stem surface is directly visible to the scanner and, the more likely it is that it remains occluded by other trees. Then, after being detected from the point clouds, successful tree height measurements require that the top of tree crowns have been visible to the scanner, and that the tree crowns have been delineated correctly. The use of intensive thinnings led to sparser forests with improved visibility to the treetops, more clearly separable tree crowns, and a smaller number of trees on lower canopy layers (see Fig. 3). Thus, tree height measurements were more accurate and the estimates remained more consistent for intensively thinned sample plots (Fig. 4).

Accuracy and consistency in tree detection and characterization led to small variation at plot-level forest structural attributes. By definition, TPH, G, and V_{mean} are computed by summing up the respective tree level attributes at plot level and thus, the accuracy of those estimates is linked with the accuracy in tree detection and tree attribute measurements. It is crucial to detect all trees from sample plots to extract unbiased estimates for TPH. In addition, dbh measurements should be accurate to ensure high accuracy for G estimates. On top of that, accurate V_{mean} estimates require that stem taper curves are estimated accurately

for reliable stem volume estimates which in turn requires accurate tree height measurements. The other plot-level forest structural attributes, D_g and H_g are less sensitive to accurate tree detection as they are computed as a weighted mean of tree attributes. With accurate dbh and tree height measurements, D_g and H_g can be estimated accurately even with a rather poor tree detection rate especially if the tree size distribution of detected trees represent the actual tree size distribution. These fundamentals in plot-level forest characterization can be seen in the results of this study (Fig. 4) as lower tree detection rate and tree height measurement accuracy are causing bias to TPH, G, and V_{mean} especially for control plots.

Performance of the TLS-based method in characterizing managed forest stands varied depending on the forest structure, which was caused by different controlled thinning treatments in our study. The accuracy measures varied differently also among sample plots with similar thinning treatments. The differences are explained by the behaviour of the TLS-based method when the forest structure varies. Thinning treatments shaped the tree size distributions causing variation in both vertical and horizontal forest structure (Figs. 2-3). Most of the trees that remained undetected were suppressed trees, and the accuracy in dbh and tree height measurements were lower for them. Thus, it is reasonable to assume that increase in the proportion of suppressed trees indicates declined overall accuracy of the TLS-based method in Scots pine stands. The proportion of suppressed trees increased when tree size variation increased, which explains the variation in the accuracy measures between different thinning treatments. The less there was variation in tree size distribution, the forest structure was more similar between the sample plots where the same thinning treatment had been applied. Therefore, more consistent results were obtained for sample plots with less tree size variation. To sum up, the results of this study support the earlier findings by (Liang et al., 2018; Yrttimaa, Saarinen, Kankare, et al., 2019) that high accuracy in TLS-based forest characterization is guaranteed for forest stands with low degree of tree size variation.

In general, consistent accuracy was obtained with the TLS-based method when estimating the forest structural attributes for thinned forest stands. Thinning intensity was noticed to have more effect on the accuracy than thinning type, which emphasizes the link between forest density and performance of the TLS-based method. Differences in accuracy between the different thinning types were minor and not considered relevant, which demonstrates that implementing different thinning types to similar forest stands did not eventually change the horizontal and vertical forest structure so much that it would considerably affect the tree detection, dbh measurement, and tree height measurement accuracy. All the tree size distributions were unimodal and only the mean and standard deviation of the distributions differed between the treatments (Figs. 2-3). At the age of around 50 years, the investigated forest stands are still growing and thus differences in the tree size distributions may be more distinct after another ten years. However, the results of this study demonstrate that higher accuracy is expected to be obtained with the TLS-based method if the overall density of trees and especially the proportion of suppressed trees is decreased with thinnings.

CONCLUSIONS

In this study we examined how forest structure affects TLS-based forest characterization by using state-of-the-art point cloud processing techniques to sample plots with controlled variation in forest structure. Based on the results of this study, we conclude that high accuracy in detecting trees, measuring tree attributes, and estimating forest structural attributes as well as tree size distributions was achieved when using the TLS-based method on managed Scots pine stands where forest management activities had been carried out. Number of trees per hectare and the proportion of suppressed trees were recognized as the main factors affecting the accuracy of TLS-based forest characterization, and those factors can typically be controlled in managed forests. Thinning decreased variation in horizontal and vertical forest structure which favours TLS-based tree detection and tree height measurement, enabling reliable estimates for forest structural attributes.

The more variation there is in the tree size distribution, the more challenging it is for the TLS-based method to capture all the trees and measure the tree attributes and forest structural attributes reliably. In general, consistent performance can be expected when using the TLS-based method in characterizing managed

forest stands. Significantly lower performance was recorded for control plots where no treatments had been carried out. Thinning intensity was noticed to have more effect on the accuracy of TLS-based forest characterization than thinning type. The use of intensive thinnings resulted in spacious canopy structure which reduced errors in tree height measurements due to improved visibility from the scanner to the treetops. Intensive thinnings also decreased the variation in tree size distribution and thus enabled more consistent forest characterization using TLS.

ACKNOWLEDGEMENTS

This research was funded by the Academy of Finland, grant numbers 315079 (“The effects of stand dynamics on tree architecture of Scots pine trees”) and 272195 (“Centre of Excellence in Laser Scanning Research”).

DECLARATION OF INTEREST

The authors declare no conflict of interest.

REFERENCES

Abegg, M., Kükenbrink, D., Zell, J., Schaepman, M., & Morsdorf, F. (2017). Terrestrial Laser Scanning for Forest Inventories—Tree Diameter Distribution and Scanner Location Impact on Occlusion. In *Forests* (Vol. 8, Issue 6, p. 184). https://doi.org/10.3390/f8060184

Åkerblom, M., Raumonen, P., Kaasalainen, M., & Casella, E. (2015). Analysis of Geometric Primitives in Quantitative Structure Models of Tree Stems. In *Remote Sensing* (Vol. 7, Issue 4, pp. 4581–4603). https://doi.org/10.3390/rs70404581

Aschoff, T., Thies, M., & Spiecker, H. (2004). Describing forest stands using terrestrial laser-scanning. *International Archives of Photogrammetry, Remote Sensing and Spatial Information Sciences*, *35*(5), 237–241.

Bauwens, S., Bartholomeus, H., Calders, K., & Lejeune, P. (2016). Forest Inventory with Terrestrial LiDAR: A Comparison of Static and Hand-Held Mobile Laser Scanning. In *Forests* (Vol. 7, Issue 12, p. 127). https://doi.org/10.3390/f7060127

Cabo, C., Ordóñez, C., López-Sánchez, C. A., & Armesto, J. (2018). Automatic dendrometry: Tree detection, tree height and diameter estimation using terrestrial laser scanning. In *International Journal of Applied Earth Observation and Geoinformation* (Vol. 69, pp. 164–174). https://doi.org/10.1016/j.jag.2018.01.011

Dassot, M., Constant, T., & Fournier, M. (2011). The use of terrestrial LiDAR technology in forest science: application fields, benefits and challenges. In *Annals of Forest Science* (Vol. 68, Issue 5, pp. 959–974). https://doi.org/10.1007/s13595-011-0102-2

Hackenberg, J., Morhart, C., Sheppard, J., Spiecker, H., & Disney, M. (2014). Highly Accurate Tree Models Derived from Terrestrial Laser Scan Data: A Method Description. In *Forests* (Vol. 5, Issue 5, pp. 1069–1105). https://doi.org/10.3390/f5051069

Heinzel, J., & Huber, M. (2016). Detecting Tree Stems from Volumetric TLS Data in Forest Environments with Rich Understory. In *Remote Sensing* (Vol. 9, Issue 1, p. 9). https://doi.org/10.3390/rs9010009

Isenburg, M. (2019). *LAStools—Efficient LiDAR Processing Software, (version 181001 academic); rapidlasso GmbH: Gilching, Germany*. http://rapidlasso.com/LAStools

Junttila, S., Holopainen, M., Vastaranta, M., Lyytikäinen-Saarenmaa, P., Kaartinen, H., Hyyppä, J., & Hyyppä, H. (2019). The potential of dual-wavelength terrestrial lidar in early detection of Ips typographus (L.) infestation – Leaf water content as a proxy. In *Remote Sensing of Environment* (Vol. 231, p. 111264). https://doi.org/10.1016/j.rse.2019.111264

Koreň, M., Mokroš, M., & Bucha, T. (2017). Accuracy of tree diameter estimation from terrestrial laser

scanning by circle-fitting methods. In *International Journal of Applied Earth Observation and Geoinformation* (Vol. 63, pp. 122–128). https://doi.org/10.1016/j.jag.2017.07.015

Laasasenaho, J. (1982). *Männyn, Kuusen Ja Koivun Runkokäyrä- Ja Tilavuusyhtälöt*.

Liang, X., Hyyppä, J., Kaartinen, H., Lehtomäki, M., Pyörälä, J., Pfeifer, N., Holopainen, M., Brolly, G., Francesco, P., Hackenberg, J., Huang, H., Jo, H.-W., Katoh, M., Liu, L., Mokroš, M., Morel, J., Olofsson, K., Poveda-Lopez, J., Trochta, J., … Wang, Y. (2018). International benchmarking of terrestrial laser scanning approaches for forest inventories. In *ISPRS Journal of Photogrammetry and Remote Sensing* (Vol. 144, pp. 137–179). https://doi.org/10.1016/j.isprsjprs.2018.06.021

Liang, X., Kankare, V., Hyyppä, J., Wang, Y., Kukko, A., Haggrén, H., Yu, X., Kaartinen, H., Jaakkola, A., Guan, F., Holopainen, M., & Vastaranta, M. (2016). Terrestrial laser scanning in forest inventories. In *ISPRS Journal of Photogrammetry and Remote Sensing* (Vol. 115, pp. 63–77). https://doi.org/10.1016/j.isprsjprs.2016.01.006

Liang, X., Litkey, P., Hyyppa, J., Kaartinen, H., Vastaranta, M., & Holopainen, M. (2012). Automatic Stem Mapping Using Single-Scan Terrestrial Laser Scanning. In *IEEE Transactions on Geoscience and Remote Sensing* (Vol. 50, Issue 2, pp. 661–670). https://doi.org/10.1109/tgrs.2011.2161613

Luoma, V., Saarinen, N., Wulder, M., White, J., Vastaranta, M., Holopainen, M., & Hyyppä, J. (2017). Assessing Precision in Conventional Field Measurements of Individual Tree Attributes. In *Forests* (Vol. 8, Issue 2, p. 38). https://doi.org/10.3390/f8020038

Maas, H. -G, -G. Maas, H., Bienert, A., Scheller, S., & Keane, E. (2008). Automatic forest inventory parameter determination from terrestrial laser scanner data. In *International Journal of Remote Sensing* (Vol. 29, Issue 5, pp. 1579–1593). https://doi.org/10.1080/01431160701736406

Meyer, F., & Beucher, S. (1990). Morphological segmentation. In *Journal of Visual Communication and Image Representation* (Vol. 1, Issue 1, pp. 21–46). https://doi.org/10.1016/1047-3203(90)90014-m

Newnham, G. J., Armston, J. D., Calders, K., Disney, M. I., Lovell, J. L., Schaaf, C. B., Strahler, A. H., & Mark Danson, F. (2015). Terrestrial Laser Scanning for Plot-Scale Forest Measurement. In *Current Forestry Reports* (Vol. 1, Issue 4, pp. 239–251). https://doi.org/10.1007/s40725-015-0025-5

Olofsson, K., & Holmgren, J. (2016). Single Tree Stem Profile Detection Using Terrestrial Laser Scanner Data, Flatness Saliency Features and Curvature Properties. In *Forests* (Vol. 7, Issue 12, p. 207). https://doi.org/10.3390/f7090207

Popescu, S. C., & Wynne, R. H. (2004). Seeing the Trees in the Forest. In *Photogrammetric Engineering & Remote Sensing* (Vol. 70, Issue 5, pp. 589–604). https://doi.org/10.14358/pers.70.5.589

Rantala, S. (Ed.). (2011). *Finnish forestry practice and management*. Metsäkustannus, Helsinki.

Raumonen, P., Kaasalainen, M., Åkerblom, M., Kaasalainen, S., Kaartinen, H., Vastaranta, M., Holopainen, M., Disney, M., & Lewis, P. (2013). Fast Automatic Precision Tree Models from Terrestrial Laser Scanner Data. In *Remote Sensing* (Vol. 5, Issue 2, pp. 491–520). https://doi.org/10.3390/rs5020491

Ritter, T., Schwarz, M., Tockner, A., Leisch, F., & Nothdurft, A. (2017). Automatic Mapping of Forest Stands Based on Three-Dimensional Point Clouds Derived from Terrestrial Laser-Scanning. In *Forests* (Vol. 8, Issue 8, p. 265). https://doi.org/10.3390/f8080265

Saarinen, N., Kankare, V., Vastaranta, M., Luoma, V., Pyörälä, J., Tanhuanpää, T., Liang, X., Kaartinen, H., Kukko, A., Jaakkola, A., Yu, X., Holopainen, M., & Hyyppä, J. (2017). Feasibility of Terrestrial laser scanning for collecting stem volume information from single trees. In *ISPRS Journal of Photogrammetry and Remote Sensing* (Vol. 123, pp. 140–158). https://doi.org/10.1016/j.isprsjprs.2016.11.012

Saarinen, N., Kankare, V., Yrttimaa, T., Viljanen, N., Honkavaara, E., Holopainen, M., Hyyppa, J., Huuskonen, S., Hynynen, J., & Vastaranta, M. (2020). Assessing the effects of stand dynamics on stem growth allocation of individual Scots pine trees. In *bioRxiv* (p. 2020.03.02.972521). https://doi.org/10.1101/2020.03.02.972521

Wang, Y., Lehtomäki, M., Liang, X., Pyörälä, J., Kukko, A., Jaakkola, A., Liu, J., Feng, Z., Chen, R., &

Hyyppä, J. (2019). Is field-measured tree height as reliable as believed – A comparison study of tree height estimates from field measurement, airborne laser scanning and terrestrial laser scanning in a boreal forest. In *ISPRS Journal of Photogrammetry and Remote Sensing* (Vol. 147, pp. 132–145). https://doi.org/10.1016/j.isprsjprs.2018.11.008

Wilkes, P., Lau, A., Disney, M., Calders, K., Burt, A., de Tanago, J. G., Bartholomeus, H., Brede, B., & Herold, M. (2017). Data acquisition considerations for Terrestrial Laser Scanning of forest plots. In *Remote Sensing of Environment* (Vol. 196, pp. 140–153). https://doi.org/10.1016/j.rse.2017.04.030

Yrttimaa, T., Saarinen, N., Kankare, V., Liang, X., Hyyppä, J., Holopainen, M., & Vastaranta, M. (2019). Investigating the Feasibility of Multi-Scan Terrestrial Laser Scanning to Characterize Tree Communities in Southern Boreal Forests. In *Remote Sensing* (Vol. 11, Issue 12, p. 1423). https://doi.org/10.3390/rs11121423

Yrttimaa, T., Saarinen, N., Luoma, V., Tanhuanpää, T., Kankare, V., Liang, X., Hyyppä, J., Holopainen, M., & Vastaranta, M. (2019). Detecting and characterizing downed dead wood using terrestrial laser scanning. In *ISPRS Journal of Photogrammetry and Remote Sensing* (Vol. 151, pp. 76–90). https://doi.org/10.1016/j.isprsjprs.2019.03.007

Zhang, W., Wan, P., Wang, T., Cai, S., Chen, Y., Jin, X., & Yan, G. (2019). A Novel Approach for the Detection of Standing Tree Stems from Plot-Level Terrestrial Laser Scanning Data. In *Remote Sensing* (Vol. 11, Issue 2, p. 211). https://doi.org/10.3390/rs11020211